Biochimica et Biophysica Acta, 443 (1976) 339–347

BBA 77410

STANDING-GRADIENT OSMOTIC FLOW

EXAMINATION OF ITS VALIDITY USING AN ANALYTICAL METHOD

JONG J. LIM[b] and JORGE FISCHBARG[a,b]

Departments of Physiology[a] and Ophthalmology[b], College of Physicians and Surgeons, Columbia University, New York, N.Y. 10032 (U.S.A.)

(Received January 27th, 1976)

SUMMARY

The solutions to the non-linear differential equations governing solute-solvent coupling in the intercellular spaces of epithelial layers have been obtained by using an analytical method, rather than the usual numerical ones. When the present series solution includes second-order correction terms, the concentration and velocity profiles obtained by the analytical method agree very well with those coming from numerical solutions. This method has further allowed us to examine the standing-gradient hypothesis when applied to the backwards fluid transport system of the corneal endothelium. With the information presently available for the relevant parameters (osmotic permeability, rate of transport, radius and length of the spaces, and location of the pumping sites), near-isotonicity of the transported fluid would not be explained by the standing-gradient model.

INTRODUCTION

A well-known explanation for the mechanism of solute-solvent coupling that results in fluid transport in epithelia has been provided by the theory of standing-gradient osmotic flow. Diamond and Bossert [1, 2], who quantitatively formulated it have dealt with both the forwards and backwards cases. Before the formal formulation of this theory was advanced, a model similar to the forwards case based on the existence of local osmosis in long and narrow channels had been proposed by Heinz [3] and later by Diamond [4]. The differential equation governing solvent flow in terms of their model is a third-order non-linear one. For this reason, it has been solved by using a numerical method on a digital computer [1, 2] or by analog computation [5]. Another procedure adopted has however been to linearize this equation by the application of a perturbation method [6]. Using what he branded as an isotonic convection approximation, Segel [6] obtained the first order solution to this differential equation for the forwards case. Although he obtained the second-order solution in an Appendix for the forwards case, Segel did not take into account this second-order correction in detail in his report. Furthermore, the second-order solutions for the velocity given in that Appendix appear to suffer from an omission, since a term in x^2 should be present in the solution (see eqn. 11 below). In the present communication we report that, by extending his procedure to include this second-order approximation in detail, the solutions obtained for both the forwards and the backwards cases give excellent agreement in comparison with results obtained by numerical methods. This method has further allowed us to examine in detail the standing-gradient theory as an explanation for fluid transport in the particular case of the corneal endothelium.

THEORY AND RESULTS

Following the procedure used by Segel [6] for the forwards case, the differential equations governing the backwards case are written as follows (cf. ref. 7 for the general theory of perturbation analysis):

$$\nu k^2 C v - \lambda^2 \mathrm{d}C/\mathrm{d}x = -k^2 \nu \begin{pmatrix} x \\ 1 \end{pmatrix}$$

for $0 \leqslant x \leqslant 1$ (1a)

and

for $1 < x \leqslant \lambda$ (1b)

$$(C-1) = \nu \mathrm{d}v/\mathrm{d}x \qquad (2)$$

where $\nu = N_0/C_0^2 P$; $k^2 = 2\, C_0 P L^2/rD$; $\lambda = L/d$;

N_0 = the solute output rate per unit area of intercellular channel wall, which is assumed to be uniform; v = the velocity of fluid at the point x in the channel; P = the osmotic permeability of the channel wall; C, C_0 = the concentrations of solute at the point x in the channel and in the ambient solution, respectively; d = the length of the solute pumping region assumed to be located at the closed end of the channel; D = the diffusion constant of the solute; L = the length of the channel; and r = the radius of the channel. The geometry of the system is assumed to be that of a cylinder with one end closed and the other end open. The boundary conditions used are as follows:

(a) At $x = 0$, $v = 0$ or $\mathrm{d}c/\mathrm{d}t = 0$ (3)

(b) At $x = \lambda$, $C/C_0 = 1$ (4)

(c) At $x = 1$, C and v are continuous (5)

It should be noted that the boundary conditions and the form of the differential equations have not been changed from the ones used by others [1, 2, 6] because it is intended in this study to compare the results obtained by two approaches: numerical and analytical. It should be also noted that the boundary conditions Eqns. 3 and 5 in particular are not in conformity with the available experimental data presently available; in all likelihood, at $x = 0$, $v \neq 0$, since the intercellular junctions are permeable to molecules as large as horseradish peroxidase [8] and presumably also to water. Similarly, the continuity conditions at the boundary $x = 1$ need not be included since the evidence points to the existence of transporting sites uniformly along the channel [9]. Letting the solution to the differential equation be the sum of terms with the perturbation parameter ν as the expansion coefficient and $C^{(j)}$ and $v^{(j)}$ as variables, the differential equations are linearized by collecting the terms with the same power of ν and can be integrated easily.

The first order solutions obtained are as follows:

$$C_{\rm I}^{(1)}(x) = A_1 \cosh kx/\lambda - 1 \tag{6}$$

$$v_{\rm I}^{(0)}(x) = \lambda/kA_1 \sinh kx/\lambda - x \tag{7}$$

for a region I, where the active transporting sites would be situated, and

$$C_{\rm II}^{(1)}(x) = -A_2 \cosh k(1-x/\lambda) \tag{8}$$

$$v_{\rm II}^{(0)}(x) = \lambda/k\ A_2 \cosh k(1-x/\lambda) - 1, \tag{9}$$

for a region II, where there would be no transporting sites. In the equations above, $A_1 = \cosh k(1-1/\lambda)/\cosh k$ and $A_2 = \sinh k/\lambda/\cosh k$.

The plots of the first order solutions for the forwards (see ref. 6) and backwards cases are shown in Figs. 1 and 2 respectively. For curve 4 in Fig. 1 and curve 1 in Fig. 2, the agreement between the first order calculation and the computer calculations [1, 2] also shown in those figures is excellent. Higher order corrections however appear to be needed for the rest of the curves. In order to achieve this, a second order correction can in turn be obtained by solving the equation

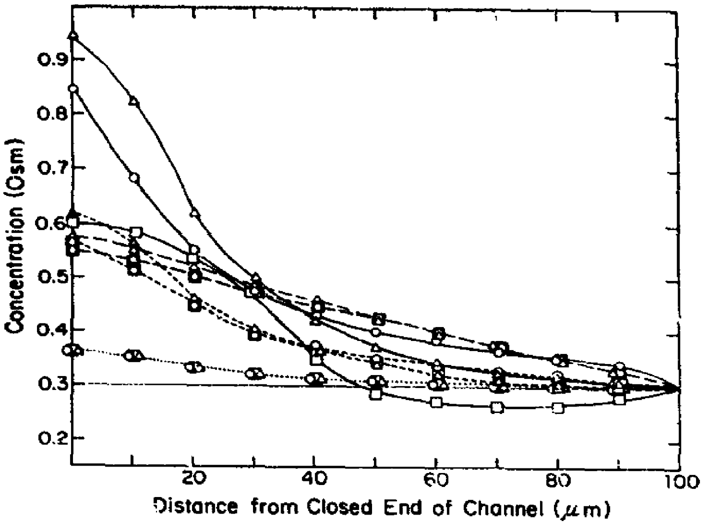

Fig. 1. Comparison of the concentration profiles obtained by an analytical method (present study) with the ones obtained by Diamond and Bossert [1, 2] for the forwards system. The solid lines represent curve 1, the long broken lines curve 2, the short broken lines curve 3, and the dotted line curve 4 of Diamond and Bossert. The triangle, square, and circle represent, respectively, the curves predicted by the first-order term, first- plus second-order terms (of the series of solutions to the differential equation), and those of Diamond and Bossert. The light solid line at 0.3 osM. indicates the ambient osmolarity.

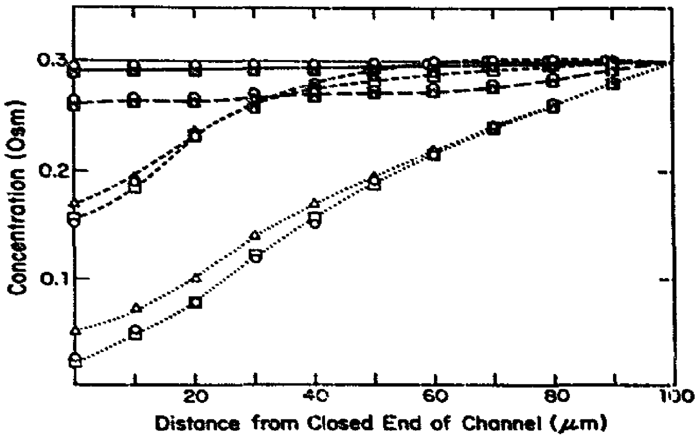

Fig. 2. Comparison between the results of the present study and the ones reported by Diamond and Bossert [2] for the backwards system. The lines and symbols represent the same curves as Fig. 1.

$$\lambda^2 v^{(0)''} - k^2 v^{(1)} = k^2 v^{(0)} C^{(1)} \tag{10}$$

For region I, substitution of Eqns. 6 and 7 into Eqn. 10 gives

$$\lambda^2 v^{(1)''} - k^2 v^{(1)} = k^2 (A_1 \cosh kx/\lambda - 1)(\lambda/kA_1 \sinh kx/\lambda - 1)$$

The solution of this equation is:

$$\begin{aligned} v_I^{(1)} = {} & B_1 \cosh kx/\lambda + C_1 \sinh kx/\lambda - x - k/4\lambda\, A_1 \chi^2 \sinh kx/\lambda - A_1/4\, x \cosh kx/\lambda \\ & + \lambda/k\, A_1^2/6 \sinh 2\, kx/\lambda \end{aligned} \tag{11}$$

and by differentiation,

$$\begin{aligned} C_I^{(2)}(x) = {} & k/\lambda (B_1 \sinh kx/\lambda + C_1 \cosh kx/\lambda - A_1/2\, x \sinh kx/\lambda \\ & - A_1/4 (k/\lambda) x^2 \cosh kx/\lambda - A_1/4\, x \sinh kx/\lambda) \\ & - A_1/4 \cosh kx/\lambda + A_1^2/3 \cosh 2\, kx/\lambda - 1 \end{aligned} \tag{12}$$

Eqn. 11 should be compared with the one given in Appendix B (Segel, ref. 6). By substituting $v_{II}^{(0)}$ and $C_{II}^{(1)}$ into Eqn. 10, and using the same procedure as with Eqns. 11 and 12, one has

$$\begin{aligned} v_{II}^{(1)}(x) = {} & B_2 \cosh kx/\lambda + C_2 \sinh kx/\lambda - \lambda/k (A_2^2/6) \sinh 2\, k(1 - x/\lambda) \\ & - (k/\lambda)(A_2/2) x \cosh k(1 - x/\lambda) \end{aligned} \tag{13}$$

and

$$\begin{aligned} C_{II}^{(2)}(x) = {} & k/\lambda (B_2 \cosh kx/\lambda + C_2 \cosh kx/\lambda) + A_2^2/3 \cosh 2\, k(1 - x/\lambda) \\ & - (k/\lambda)(A_2/2) \cosh k(1 - x/\lambda) + (A_2/2)(k/\lambda) x \sinh k\, (1 - x/\lambda) \end{aligned} \tag{14}$$

The constants B_1, C_1, B_2 and C_2 are obtained by using the boundary conditions, Eqns. 3, 4 and 5; they are as follows: $B_1 = 0$,

$$
\begin{aligned}
k/\lambda B_2 = {} & A_2^2/3 \sinh k/\lambda \cosh 2\, k(1-1/\lambda) + A_2^2/6 \cosh k/\lambda \sinh 2\, k(1-1/\lambda) \\
& + (k/\lambda)^2 (A_2/2) \cosh k - (k/\lambda)(A_2/2) \sinh k/\lambda \cosh k\, (1-1/\lambda) \\
& + (k/\lambda)(A_1/2) (\sinh k/\lambda)^2 - (k/\lambda) A_1/4 + A_1/4 \cosh k/\lambda \sinh k/\lambda \\
& - A_1^2/3 \sinh k/\lambda \cosh 2\, k/\lambda + \sinh k/\lambda - k/\lambda \cosh k/\lambda + A_1^2/6 \cosh k/\lambda \sinh 2k/\lambda,
\end{aligned}
$$

and

$$
\begin{aligned}
C_2 = {} & A_2/\cosh k\, (\tfrac{1}{2} - A_2/3\, (\lambda/k)) - \tanh k\, B_2, \text{ and } C_1 \cosh k/\lambda = 3\, A_1/4 \\
& \sinh k/\lambda + A_1/4\, (k/\lambda) \cosh k/\lambda + B_2 \sinh k/\lambda \\
& + C_2 \cosh k/\lambda + \lambda/k\, A_2^2/3 \cosh 2k(1-1/\lambda) - A_2/2 \cosh k(1-1/\lambda) \\
& + A_2/2(k/\lambda) \sinh k\, (1-1/\lambda) + \lambda/k\, (A_1/4 \cosh k/\lambda - A_1^2/3 \cosh 2\, k/\lambda + 1).
\end{aligned}
$$

It may be noted that when ν is small, higher order terms can be neglected. The solutions including the second order correction terms are as follows:

$$v(x, \nu) = v^{(0)} + \nu v^{(1)} \tag{15}$$

$$C(x, \nu) = 1 + \nu C^{(1)} + \nu^2 C^{(2)} \tag{16}$$

Some of the results that can be obtained with these solutions are also shown in figs. 1 and 2, together with the ones obtained through computer calculations by Diamond and Bossert [1, 2]. In order to test our solutions, we have used the same values for the parameters as employed by Diamond and Bossert [1, 2]. It can be clearly seen that with the second-order correction the comparison is excellent for curves 2, 3, and 4 in Fig. 1. Curve 1 of Diamond and Bossert [1] appears however to agree better with the first-order than with the second-order solution. An explanation for this discrepancy might come from the fact that the solutions obtained (Eqns. 15 and 16) are functions of both k and ν, which in turn are dependent on parameters such as permeability (P) and rate of transport (N_0). Both k and ν for curve 1 are large (see Table I) compared with the parameters used for the rest of the curves. As a result, the second order correction is large, and higher order corrections seem to be needed. All backwards concentration profiles are shown in Fig. 2. Since there is no term where both k and ν are large, it is seen that the agreement between our results and that of Diamond and Bossert [2] is excellent. From the comparison made so far between the analytical and numerical methods, it is clear that no terms higher than second-order corrections are needed for the cases considered except the one discussed above. Consequently, it appears that no elaborate time consuming computer analysis is required for the gradient analysis. The solutions given by Segel [6] and by us in this report should suffice in order to obtain the concentration and velocity profiles linked to epithelial fluid transport.

Another important parameter associated with the standing-gradient osmotic theory is the osmolarity of the emergent fluid, which is given by;

$$\bar{O}_s = c \int_0^d \bar{N}(\bar{x}) \mathrm{d}\bar{x} / a\bar{v}(L) = C_0/v(L) \tag{17}$$

the normalized osmolarity is given by;

$$O_s = \bar{O}_s/C_0 = 1/v(L)$$

TABLE I

COMPARISON OF CONCENTRATIONS OF THE TRANSPORTED FLUID OBTAINED BY DIFFERENT APPROACHES

See text for the other parameters.

Curve* #	k	ν	P(cm/s per osM)	N_0(mosM/cm per s)	Osmolarity of the emergent fluid			
					**	*	This study	
							First-order	First-+second-order
Forwards								
1	4.9	5.56	$2 \cdot 10^{-5}$	10^{-5}	0.420	0.342	0.305	0.327
2	1.095	11.1	10^{-6}	10^{-6}	1.08	0.803	0.756	0.818
3	4.9	2.778	$2 \cdot 10^{-5}$	$5 \cdot 10^{-6}$	0.380	0.318	0.305	0.316
4	4.9	0.56	$2 \cdot 10^{-5}$	10^{-6}	0.301	0.304	0.305	0.327
						Osmolarity of the transported fluid		
						*	This study	
							First-order	First-+second-order
Backwards								
1	6.928	$3.083 \cdot 10^{-2}$	$4.0 \cdot 10^{-5}$	$1.11 \cdot 10^{-7}$	–	0.322	0.326	0.323
2	3.464	$1.389 \cdot 10^{-1}$	10^{-5}	$1.25 \cdot 10^{-7}$	–	0.352	0.366	0.362
3	4.900	1.111	$2 \cdot 10^{-5}$	$2 \cdot 10^{-6}$	–	0.300	0.305	0.301
4	1.549	$1.533 \cdot 10^{-3}$	$2 \cdot 10^{-6}$	$1.15 \cdot 10^{-6}$	–	0.455	0.507	0.464

* Diamond and Bossert refs. 1 and 2.

** Hempling, ref. 5.

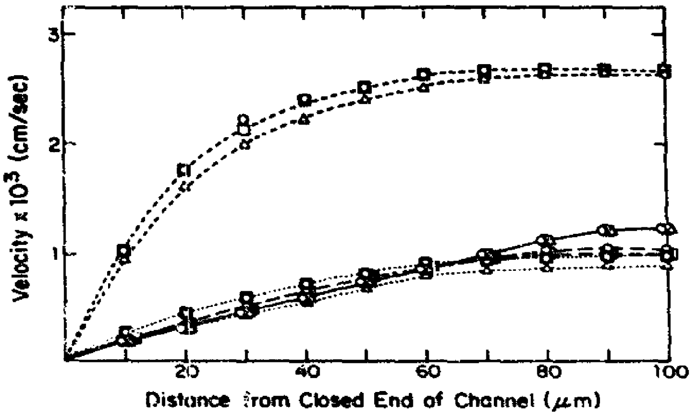

Fig. 3. Plots of the velocity profiles of the backwards system as a function of the distance from the closed end of the channel. The lines and the symbols are as defined as in Fig. 1.

The normalized osmolarity is dependent only on the velocity at the open end of the channel, as shown above. The velocity profiles for the backwards case [2] are shown in Fig. 3. In Table I we compare presently calculated osmolarity values with those coming from previous procedures (Diamond and Bossert, numerical analysis solution on a digital computer [1, 2]; Hempling, solution on an analog computer [5]). It can be seen that Hempling's results are somewhat higher than those of Diamond and Bossert or ours. The close agreement between Diamond and Bossert's and our data shows that both numerical and perturbation analysis can yield similar detailed information regarding the standing-gradient osmotic profiles. It appears that the analytical method depicted here is accurate enough, and simpler and much less time-consuming in comparison with the numerical methods.

DISCUSSION

The procedure presently reported has been further used in order to examine a central question regarding the standing-gradient model. Hill [10] has recently raised questions as to the feasibility of the standing-gradient theory for explaining osmotic flow in epithelia based on the fact that, as he reported it, the value of the osmotic permeability should be greater than the values experimentally measured by two orders of magnitude in order to explain isotonic flow of solute under all conditions. If extrapolated, this assertion would be also valid for the case of the corneal endothelial preparation that we have examined here in detail. For this backwards system with parameters: $D = 1.54 \times 10^{-5}$ cm²/s; $r = 1.5 \times 10^{-6}$ cm; $C_0 = 0.3$ osM; $L = 12 \times 10^{-4}$ cm; $N_0 = 8.5 \times 10^{-8}$ mosM/cm² per s; $P = 4.8 \times 10^{-5}$ cm/s per osM, the plots of osmolarity of the transported fluid (from Eq. 17) as a function of permeability are depicted in Fig. 4 for two cases: (a) pumps restricted to the 1/10 of the channel length nearest to the closed end ($\lambda = 10$) (cf. refs. 1, 2), (b) pumps uniformly distributed along the channel ($\lambda = 1$) (cf. ref. 10). As shown in Fig. 4, the fluid transported comes out to be hypertonic for either case, by a factor of about 3 and 2 for the $\lambda = 1$ and the $\lambda = 10$ cases respectively. This might be a reflection of the fact that the

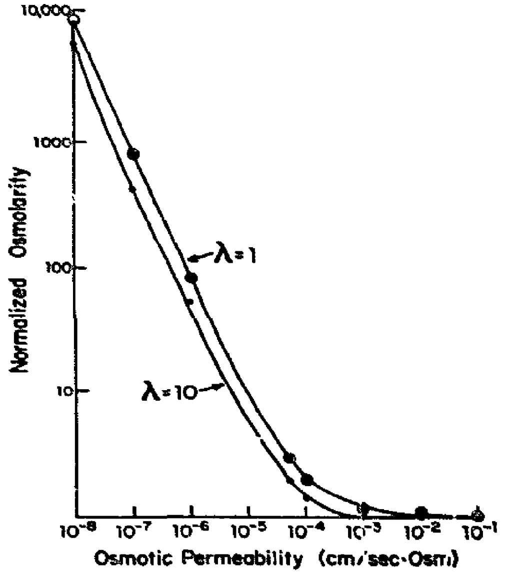

Fig. 4. Normalized osmolarity vs. osmotic permeability. $\lambda = 1$, and $\lambda = 10$ correspond respectively to the cases in which the transporting sites are assumed to be located uniformly along the entire channel length and along one-tenth of the length from the closed end of the channel. Increasing λ above 10 does not shift the curve measurably from the case of $\lambda = 10$.

length of the corneal endothelium intercellular channel is comparatively short (approx. 12 μm), which is substantially less than the channel lengths considered for other fluid transporting epithelia. In order to achieve isotonic flow in this preparation with the parameters above, the magnitude of permeability must be about 10^{-3} cm/s per osM, which is again about two orders of magnitude larger than values experimentally measured in this * and other similar tissues. In this, the present results agree with similar contentions recently made by Hill [10]. The only alternative way to achieve isotonic flow with the observed values for osmotic permeability would be to increase the length and/or decrease the radius of the channel. Since the permeability needed for isotonic transport would be about 100-times larger than the one experimentally measured*, the ratio $\sqrt{L^2/r}$ in the parameter k must be 10^2 to compensate for the high value of the osmotic permeability. The value for the radius (1.5×10^{-6} cm) used in the above estimate is the smallest one observed in electron micrographs [11]. The value of L (12×10^{-4} cm) used here takes into account the tortuosity of the channel, and should therefore be considered as the maximum possible value. Calculations from recent measurements* further suggest that the fluid transported by the endothelium would not be far from isotonic. Though the discrepancy involved is not large, in view of the present evidence, it appears that the standing-gradient theory for osmotic flow as originally formulated might not quite explain near-isotonic fluid transport in this preparation. Either a modified theory or alternative models, such as the double membrane one [12, 13], electro-osmosis [10] or pinocytosis would also deserve careful consideration.

---

* Fischbarg, J. and Lim, J. J., in preparation.

ACKNOWLEDGEMENTS

This work was supported by U.S.P.H.S. Research Grants (EY 00727, EY 01080) and Research Career Development Award EY 00006 to Dr. Fischbarg, by Grant EY 01422 to Dr. Lim, and in part by Fight for Sight, Inc., New York City.

REFERENCES

1 Diamond, J. M. and Bossert, W. H. (1967) J. Gen. Physiol. 50, 2061–2083
2 Diamond, J. M. and Bossert, W. H. (1968) J. Cell Biol. 37, 694–702
3 Heinz, V. E. (1960) Klin. Physiol. 1, 184–203
4 Diamond, J. M. (1964) J. Gen. Physiol. 48, 15–42
5 Hempling, H. G. (1968) J. Gen. Physiol. 51, 273–276
6 Segel, L. A. (1970) J. Theor. Biol. 29, 233–250
7 Nayfeh, A. (1973) Perturbation Methods, pp. 2–6, John Wiley and Sons, New York
8 Kaye, G. I., Sibley, R. C. and Hoefle, F. B. (1973) Exp. Eye Res. 15, 585–613
9 Kaye, G. I. and Tice, L. W. (1966) Invest. Ophthal. 5, 22–32
10 Hill, A. E. (1975) Proc. R. Soc. Lond. B. 190, 99–114
11 Kaye, G. and Papas, G. D. (1962) J. Cell Biol. 12, 457–479
12 Patlak, C. S., Goldstein, D. A. and Hoffman, J. F. (1963) J. Theor. Biol. 5, 426–442
13 Ogilvie, J. T., McIntosh, J. R. and Curran, P. F. (1964) Biochim. Biophys. Acta 66, 441–444